Lichenysin-geminal amino acid-based surfactants: synergistic action of an unconventional antimicrobial mixture

Jonathan Coronel-León[a,b,] Aurora Pinazo[c], Lourdes Pérez[c], Mª José Espuny[a], Ana Mª Marqués[a], Angeles Manresa[a].

[a]Laboratori de Microbiologia. Facultat de Farmacia. Universitat de Barcelona. Joan XXIII s/n. 08028 Barcelona, Spain.

[b]Present adress: Escuela Superior Politécnica del Litoral, ESPOL, Facultad de Ingeniería Mecánica y Ciencias de la Producción. Campus Gustavo Galindo Km 30.5 Vía Perimetral, P.O.Box 09-01-5863, Guayaquil, Ecuador.

[c]Department of Chemical and Surfactant Technology, IQAC-CSIC, Jordi Girona18-26. 08034 Barcelona, Spain

Keywords: antimicrobial properties; lichenysin; flow cytometry; transmission electron microscopy; potassium leakage; Gemini surfactants; *Listeria nonocytogenes*; *Escherichia coli*.

Highlights: Antimicrobial properties of surfactants binary system: lichenysin-gemini aminoacid-base.

Abstract:

Recently it has been demonstrated that mixtures of oppositely charged surfactants or lipids, known as catanionic mixtures, present a wide variety of organized assemblies and aggregates with improved physicochemical properties compared to those of the individual components.. Isotherms of lichenysin-$C_3(LA)_2$ indicate a strong interaction suggesting the formation of a new "pseudo-surfactant". The antimicrobial properties of the mixture lichenysin and C_3(LA) M80:20, indicate a synergistic effect of the components. The mechanism of action on the bacterial envelope was assessed by flow cytometry and Transmission Electron Microscopy.

Introduction

The continuous emergence of bacterial strains resistant to conventional preservatives has become a major problem in recent years [1, 2] and has prompted a search for alternative preservative systems. In the search for new antimicrobial agents able to reduce resistance and toxicity with wider activity spectra, a current trend is to explore mixtures of already existing antimicrobial agents [3-6].

Recently it has been demonstrated that mixtures of oppositely charged surfactants or lipids, known as catanionic mixtures, present a wide variety of organized assemblies and aggregates with improved physicochemical and antimicrobial properties compared to those of the individual components, attributed to synergistic effects [7,8]. These results prompted us to explore mixtures of lichenysin, an anionic biosurfactant, and N^{α},N^{ω}-bis(N^{α}-lauroyl-lysine) α,ω-hexylendiamide ($C_6(LL)_2$) and N^{α},N^{ω}-bis(N^{α}-lauroyl α,ω-propylendiamide ($C_3(LA)_2$, two amino acid-based gemini cationic surfactants (Fig. 1). Lichenysin ($Lch_{AL\cdot 1.1}$) is a cyclic lipopeptide produced by *Bacillus licheniformis* similarly to surfactin, with a highly surface tension activity in water (29 mN/m) with a very low (15mg/L) critical micelle concentration (CMC) [9,10], however lichenysin did not exhibited antimicrobial activity such that of surfactin [11]. Arginine- or lysine-based gemini surfactants (Fig. 1) are highly effective in reducing surface tension (30 mN/m for $C_6(LL)_2$ and 35 mN/m for $C_3(LA)_2$), have very low CMC (~ 5 x 10^{-3} mM) and show antimicrobial activity with moderate toxicity [12-14]. Because of their high surface and antimicrobial activities, several potential biomedical therapeutic and prophylactic applications have been described for these compounds, which have drawn the attention of cosmetic, biomedical and pharmaceutical industries [8-13].

To assess the biological properties of the surfactant binary systems described, we conducted an *in vitro* evaluation of the antimicrobial activity of $Lch_{AL\cdot 1.1}$ and two gemini compounds, $C_6(LL)_2$) or $C_3(LA)_2$, alone and as mixtures, against the pathogenic strains *Escherichia coli* O157:H7 and *Listeria monocytogenes*, both considered a challenge to food security. The effect of the gemini arginine /lichenysin catanionic surfactant mixture on cell viability and on functional and structural cell integrity was investigated.

Material and methods

2.1 Synthesis and production of surface active molecules

The gemini surfactants $C_6(LL)_2$ and $C_3(LA)_2$ were synthesized and purified as reported [15-17]. Lichenysin ($Lch_{AL1.1}$), was obtained as previously described [18] . The structures of all compounds are shown in Fig. 1.

2.2 Physicochemical characterization of surface active molecules

2.2.1 π-A Compression Isotherms

To obtain surface pressure versus mean molecular area (π-A) isotherms at room temperature, a computer-controlled Langmuir balance (KSV Instruments Ltd. Helsinki) 364 mm long and 75 mm wide was used. The surface pressure was measured with a Wilhelmy plate made of filter paper (Whatman ashless, 70 mm Ø). The uncertainty of the Langmuir balance is ±0.1 mN/m. Before spreading, the surface was compressed and the top layer of the subphase aspirated with a Pasteur pipette. The surface was considered clean after checking that the pressure rise between full expansion and full compression was <0.1 mN/m. Samples were prepared by weight at a concentration of 1 mg/mL in chloroform for $C_3(LA)_2$ and $C_3(LA)_2$/ $Lch_{AL1.1}$ and in hexane/methanol (9:1) solvent for $C_6(LL)_2$ and $C_6(LL)_2$/$Lch_{AL1.1}$. Sample aliquots of 20 μL were spread onto the surface of buffer solutions of TRIS (pH 7.4). After solvent evaporation, symmetric compression of the monolayer was done at 20 mm^2/min rate. The reproducibility of the surface pressure was higher than 0.4 mN/m [19].

2.2.2 Size and zeta potential

$Lch_{AL1.1}$, $C_3(LA)_2$, and mixtures of $C_3(LA)_2$/$Lch_{AL1.1}$ (M80:20, M50:50) were prepared in concentrations of 2 mM in distilled water. The size and zeta potential of aggregates were obtained by analysing the samples in a Zetasizer Malvern Nano-ZS using a ZeNO112 cell. The value was taken as the mean of three independent measurements. Each measurement was in turn the average of ten sub-measurements of 20 s each [20].

2.3 Biological activity

2.3.1 Antimicrobial activity

The antimicrobial activity was determined on the basis of the minimum inhibitory concentration (MIC) [21]. Gemini surfactants and the binary systems were dissolved in Muller Hinton Broth (MHB, Oxoid, Basingstoke, UK,) in the concentration range of 0.1−256 μg/mL (0.1-250 μM). $Lch_{AL1.1}$ concentrations between 0.2-1024 μg/mL (0.2-1 mM) were assayed. An aliquot of 200 μL of each concentration was dispensed in the corresponding well of a 96-well polypropylene microtiter plate (Costar; Corning, NY, USA). Then, 10 μL of an overnight culture on MHB, of the corresponding microorganism were added to achieve a final concentration of 10^4-10^5 CFU/mL. Inoculated MHB served as a growth control. Microorganism growth was determined visually after 24 h incubation at 37 °C. For MIC determinations, *Escherichia coli* ATCC 25922, *Escherichia coli* O157:H7 CECT 4267, *Pseudomonas aeruginosa* ATCC 27853, *Yersinia enterocolitica* ATCC 9610, *Klebsiella pneumoniae* ATCC 13883, *Staphylococcus aureus* ATCC 29213, *Kocuria rhizophila* (previously *Micrococcus luteus*) ATCC 9341, *Bacillus subtilis* ATCC 6633, *Staphylococcus epidermis* ATCC 12228, *Listeria monocytogenes* ATCC 15313, methycillin-resistant *Staphylococcus aureus* (MRSA) ATCC 43300 and *Candida albicans* ATCC 10231 were used. Strains were subcultured fortnightly on tryptone soy agar plates (TSA, Pronadisa, Barcelona, Spain) and were preserved frozen in cryovials (EAS laboratories, France) at -80 ºC.

To evaluate the potential synergism of both surfactants assayed, the fractional inhibitory concentration (FIC) was determined according to the equation:

$$FIC = [(MIC_{AM}/MIC_A) + (MIC_{BM}/MIC_B)]$$

Where MIC_{AM} is the MIC of the geminal in the mixture, MIC_A is the MIC of the pure geminal, MIC_{BM} is the MIC of the lipopeptide in the mixture, and CMI_B is the MIC of the pure lipopeptide [22]. Differences between FIC data were analysed with the paired t-student test according to Schwartz, D. [23].

2.3.2 Exposure of E. coli O157:H7 and L. monocytogenes to the $C_3(LA)_2$ /lichenysin mixture

Microorganisms, cultured for 24h at 30ºC in TSA were washed twice (8,000 x g, 20 min; Allegra 25R, Beckman) in sterile Ringer solution (Scharlau, Barcelona, Spain). an aliquot of washed bacteria was added to peptone-buffered water (Oxoid, Basingstoke, UK) to obtain a cell density of about 10^7–10^8 CFU/mL. A volume of $C_3(LA)_2$/$Lch_{AL1.1}$ (M80:20) stock solution (2 mM) was added to flasks to reach the MIC value for *E. coli* O157:H7 and *L. monocytogenes* (6.25 µM). Single components were added at a final concentration of 5 µM for $C_3(LA)_2$ and 1.25 µM for $Lch_{AL1.1}$. The inoculated flasks were kept in darkness at room temperature.

2.3.3 Bacterial count

After exposure, samples were diluted 1:10 with sterile Ringer solution for surfactant inactivation. Bacterial viability was calculated by viable cell counts, calculated from the colony forming units (CFU/mL). Briefly, after ten-fold serial dilution of treated bacterial suspension, 0.1 mL aliquots were spread on TSA plates surface and incubated at 37ºC for 24-48 h. Control bacterial suspensions were run in parallel. Cell counting was performed per triplicate and SE was calculated. Viability was calculated as follows: B=N/d were, B: number of bacteria; N: average number of colonies counted on three plates, and d: dilution factor.

2.3.4 Analysis by flow cytometry (FC)

After 60 min exposure, cell suspensions were diluted 1:10 in PBS, centrifuged (8000 g for 20 min), washed, re-suspended in 2 mL of peptone-buffered water, Control samples without surfactant treatment were prepared in parallel. The staining protocols for FC experiments and FC analysis were reported earlier [24].

2.3.5 Potassium leakage

The potassium concentration in the supernatant was measured with an Inductively Coupled Plasma Spectrometer (ICP_OES Perkin Elmer, model 3200Rl) using standard potassium ion solutions of 0-1ppm concentrations as the reference. Experiments were conducted in triplicate, and means and standard deviations were calculated[24].

2.3.6. Observation by transmission electron microscopy (TEM)

Cell suspensions of *E. coli* O157:H7 CECT 4267 and *L. monocytogenes* ATCC 15313 were exposed for 2 h with M80:20 (6.5 μM) and with $C_3(LA)_2$ (5 μM). Untreated cells were used as controls. 50 mL samples were taken, centrifuged (8000 x g for 20 min), and the bacterial pellets were rinsed with buffered peptone water (pH 7) three times. Samples were treated as reported [15, 24]. Ultrathin sections were cut with a Leica UCT ultra microtome and mounted on Formvar carbon-coated copper grids. Sections were poststained with 2% aqueous uranyl acetate and lead citrate and examined by a Tecnai Spirit electron microscope (FEI Company, Netherlands) at an acceleration voltage of 120 kV and a computer program analySIS (Soft Imagine System, Switzerland).

3. **Results and discussion**

3.1 Surface Pressure-Area (π-A) Isotherms

The monolayer compression isotherms (π-A) of pure $Lch_{AL1.1}$, $C_3(LA)_2$, and $C_6(LL)_2$, and $C_3(LA)_2$/$Lch_{AL1.1}$ and $C_6(LL)_2$/$Lch_{AL1.1}$ mixtures at proportions of 80:20 and 50:50 are presented in Fig. 2. The shapes of the π-A isotherms of pure $C_3(LA)_2$ and $C_6(LL)_2$ show a characteristic profile of surfactants with a relatively high solubility. At subphase pH 7.4, the evaluated compounds were in ionized form. $C_3(LA)_2$ has two positive charges situated in the guanidine groups (pKa=9), and while $Lch_{AL1.1}$ has one negative charge due to the aspartic acid residue (pKa=3.5). For $C_3(LA)_2$ it was observed that, under monolayer compression, the surface pressure (Fig 2a) increased slowly over large molecular areas (gaseous phase). At 125 $Å^2$/molecule, a liquid-expanded phase was observed. With further area compression, the monolayer collapsed and the surface pressure reached a value of 26 mN/m. The isotherm profile of $C_6(LL)_2$ was similar to that $C_3(LA)_2$. The isotherm shape of a pure $Lch_{AL1.1}$ monolayer implied that this monolayer behaves as an expanded monolayer at the interface, probably related to the big head groups of these molecules. When the monolayer was compressed, the liquid-expanded state appeared at 225 $Å^2$/molecule, and then at 45 mN/m the monolayer collapsed.

The monolayers corresponding to the $C_3(LA)_2$/$Lch_{AL1.1}$ mixtures showed a similar profile, independently of the proportions (M80:20, M50:50 in Fig. 2a). If the two monolayer components are miscible at the interface, the mixed monolayer should demonstrate intermediate isotherm behaviour between that of the corresponding pure

monolayer isotherms, and accordingly the curves of the $C_3(LA)_2$/$Lch_{AL1.1}$ mixtures lie between the curves of the pure components. This behaviour suggests the formation of a pseudo trialky surfactant with three charges, two cationic from the gemini (pK = 9) and one anionic from the $Lch_{AL1.1}$ (pK = 3.5), which partly neutralized each other. The formation of the catanionic systems is strongly synergistic. A clear effect was the surface pressure at monolayer collapse, which was higher than the value for $C_3(LA)_2$ alone and similar to that of $Lch_{AL1.1}$ (45 mN/m). The collapse occurred at values of areas lower than those in the isotherm of pure $Lch_{AL1.1}$. This indicates a higher surface density in the monolayer, probably due to the minor electrostatic repulsions. As stated, the interaction between a molecule of $Lch_{AL1.1}$ with one of a gemini surfactant could lead to the formation of a "pseudo-surfactant", with a unique positive charge; one cationic charge of $C_3(LA)_2$ is neutralized by the negative charge of $Lch_{AL1.1}$,resulting in a lower repulsion of molecules. The fact that the curve shape of the isotherm mixture $C_3(LA)_2$/$Lch_{AL1.1}$ did not change when varying the ratio of surfactants in the mixture (M80:20, M50:50) can be attributed to that, in both cases, the number of "pseudo-surfactant" molecules at the interface was the same.

The π-A isotherms of the $C_6(LL)_2$/$Lch_{AL1.1}$ mixture (Fig. 2b) show a rather flat profile, which is characteristic of surfactants with high solubility and non-compressible spread monolayers. Taking into account the pKa of $C_6(LL)_2$ [20], pKa=7.8, it is expected that at pH 7.4, only 50% of $C_6(LL)_2$ molecules are ionized, and only 50% can interact with the molecules of $Lch_{AL1.1}$, and under compression conditions most of the molecules solubilise at the subphase, therefore π values at collapse (15 mN/m) were lower than those for the $C_3(LA)_2$/$Lch_{AL1.1}$ mixture.

3.2 Size and zeta potential

Surfactants form different types of aggregates, including vesicles. In order to determine what type of aggregate form the mixture of Gemini surfactants and $Lch_{AL1.1}$, two mixture proportions (80:20, 50:50) were studied, using dynamic light scattering measurements at 25ºC. To measure the aggregate size distribution, a polydispersity index

(PI), ranging from 0.0 for an entirely monodisperse sample to 1.0 for a polydisperse sample, is used. Results are shown in Table 1.

In all cases, the scattering detected size ranges corresponding to medium and large vesicles. For $C_3(LA)_2$ dispersions, the aggregate sizes ranged from 30 to 800 nm, with a major intensity at 194 nm and with a polydispersity relatively high. At concentrations higher than the CMC, the gemini surfactant $C_3(LA)_2$ forms large globular aggregates [25] that can be twisted ribbons or helical aggregates depending on the concentration [26]. For $Lch_{AL1.1}$ dispersions, a bimodal size distribution with medium values of polydispersity of microstructures was observed, with one peak at around 100 nm and another at around 500 nm. This result is fairly consistent with the results reported for surfactin dispersions [27], where a bimodal distribution was observed with an average size of 180 nm and 818 nm.

In $C_3(LA)_2/Lch_{AL1.1}$ mixtures, the incorporation of $C_3(LA)_2$ (Table 1) into $Lch_{AL1.1}$ dispersions clearly resulted in a loss of bimodality in $Lch_{AL1.1}$, favouring the formation of vesicles with an average size of about 200 nm and low polydispersity in both 80:20 (Fig. 3a) and 50:50 proportions (Fig. 3b). This confirms the strong interaction of the $C_3(LA)_2/Lch_{AL1.1}$ mixtures, as explained previously in the isotherm analysis. Size of the $C_3(LA)_2/Lch_{AL1.1}$ aggregates also changed with time (data no shown), which is fairly consistent with information recently reported for surfactin vesicles [28]. For $C_6(LL)_2/Lch_{AL1.1}$ mixtures, the sizes of the aggregates were out of the detection range.

The zeta-potential is obtained from the measurement of the electrophoretic mobility and is related to the electric charge of the vesicles. As a rule of thumb, it is considered that a system is electrostatically stable if the zeta-potential has an absolute value above 20 mV. When the zeta potential is higher than 20 mV, colloidal solutions are stable, due to repulsive interactions between aggregates bearing the same charges. Due to the negative charge on the carboxyl group, the $Lch_{AL1.1}$ vesicles show a zeta-potential of -37.6 mV (Table 1). The cationic surfactant $C_3(LA)_2$, with two positive charges on the guanidine groups, has a positive zeta potential of 49.7 mV. Notably, all the solutions had high zeta potential, which explains the stability of these dispersions. $C_3(LA)_2$ has two positive charges compared to a single negative charge of $Lch_{AL1.1}$, thus one $Lch_{AL1.1}$ molecule can neutralize only one charge of $C_3(LA)_2$. The repulsion between aggregates is not strong enough to avoid coagulation and phase separation. Although both mixtures

were positively charged, their values were slightly different, i.e. the zeta potential for 80:20 was 54 mV and 66 mV for 50:50.

Antimicrobial activity of $Lch_{AL1.1}$, gemini surfactants and the gemini surfactant/ $Lch_{AL1.1}$ binary system.

The combination of antimicrobial agents has generated great interest, since a synergistic activity may expand their range of action, prevent the emergence of resistance and reduce toxicity [4]. Catanionic mixtures of $Lch_{AL1.1}$/gemini surfactant were studied to assess if they had a synergistic antimicrobial effect [7]. It is well known that most of the *Bacillus* lipopeptides are effective antimicrobials, exhibiting MICs lower than 2 μg/mL [29], However, $Lch_{AL1.1}$ inhibitory activity against a wide variety of microorganisms was weak (Table 2, Table 3).

$C_6(LL)_2$ is a moderately effective antimicrobial agent against Gram-negative or Gram-positive bacteria (Tabe 2). The MIC found ranged between 100-200 μM except in the case of *S. epidermidis* (50 μM). Despite the weak antimicrobial activity of $Lch_{AL1.1}$ (MIC >1 mM) and its low interaction with $C_6(LL)_2$ (see compression isotherms above), the antimicrobial activity against, *M. luteus* and *B. subtilis* was enhanced when mixed with $Lch_{AL1.1}$ in both proportions tested.

Critical increase in antimicrobial activity was observed for $C_3(LA)_2/Lch_{AL1.1}$ (M80:20) against most of the bacteria assayed (Table 3). A significant reduction in MICs was observed against all Gram-negative bacteria studied Among the Gram-positive bacteria assayed (Table 3), a slight reduction in MIC was observed against *S. aureus*, *B. subtilis*, *S. epidermis*, *K. rhizophila*, and MRSA whereas relevant decrease was found in the case of *L. monocytogenes* and *C. albicans*. These results are consistent with the strong interaction of $C_3(LA)_2$ and $Lch_{AL1.1}$ observed in the isotherm.

To assess the role of synergism in the antimicrobial activity of the formulations, the FIC was calculated following equation 1. A FIC≤ 0.5 indicated synergism, while values from 0.5 to 1 indicated no synergism, between 1 and 4 was defined as indifferent, and higher than 4 indicated antagonism [3, 35]. Accordingly, the activity of the binary system of $C_6(LL)_2/Lch_{AL1.1}$ M80:20 (Table 2), except against *B. subtilis* and *K. rhizophila*, clearly

showed no synergism, which is consistent with the low interaction between the two components indicated by the isotherm.

The $C_3(LA)_2$/$Lch_{AL1.1}$ M80:20 clearly acted synergistically against most of the microorganisms assayed (Table 3) showing stronger synergy than C_6LL_2 binary system ($t= 3.1652$, 11 d.o.f. with $p<<0.05$) [23] No synergism was observed against the Gram-positive bacteria assayed (FIC >0.5), with the exception of *B. subtilis* and *K. rhizophila*. The high interaction of both compounds detected by isotherms and their ability to form aggregates could be responsible for the antimicrobial activity of this mixture against Gram-negative bacteria.

It has been reported that, in general, Gemini surfactants structures show higher activity than their single chain analogues due to the enhanced intermolecular hydrophobic interactions [38]. The different synergism obtained for $C_3(LA)_2$ and $C_6(LL)_2$ can be attributed to the different pKa values of these surfactants. Such synergistic interactions allow the use of lower dosages and can also extend the range of actuation.

Novel formulations containing antimicrobial peptides (AMPs) and cationic lipids have been proposed in order to improve the therapeutic index of AMPs and their bioavailability. In general this aproach consist on the encapsulation of the AMPs on liposomes prepared with lipids. This strategies increases fusion between liposomal AMPs and the bacterium membrane thereby increasing the antibacterial activity [30].

The scarce information in the literature on the antimicrobial behaviour of binary systems involving biosurfactants is mainly limited to their physico-chemical properties [31, 32], demonstrating the synergic effect between rhamnolipids and nisin, an antimicrobial peptide, which enhanced the effectiveness against *L. monocytogenes* [33]. Another study has demonstrated that lipopeptide V9T14, a biosurfactant produced by *Bacillus*, in association with antibiotics leads to a synergistic increase in biofilm elimination efficacy, and in some combinations leads to total eradication of *E. coli* CFT073 biofilm [3]. A synergistic action of sophorolipids and tetracycline has been described, with sophorolipids enhancing the drug action by facilitating the entry across the cell membrane, thus achieving the requisite intracellular antibiotic concentration at a low dosage [34]. These and the findings presented here provide new data on potentially useful interactions against pathogens. Importantly, the addition of $Lch_{AL1.1}$ to $C_3(LA)_2$

improved the antimicrobial action against Gram-negative bacteria, which are responsible for a large proportion of antibiotic-resistant bacterial diseases.

3.4. Effect of the $C_3(LA)_2$/$Lch_{AL1.1}$ (80:20) mixture against E. coli O157: H7 and L. monocytogenes culture viability.

In order to analyse the antimicrobial mechanism of the $C_3(LA)_2$/$Lch_{AL1.1}$ (M80:20), two microorganisms particularly problematic for the food industry, *E. coli* O157:H7 and *L monocytogenes*, were chosen. Shiga toxin-producing *E. coli* O157:H7 causes gastrointestinal infections, such as haemorrhagic colitis, and haemolytic uremic syndrome, which is life-endangering [35]. *L. monocytogenes* ATCC 15313 grows in many animal food products, affecting food safety, can cause listeriosis and may be involved in meningitis, encephalitis, septicemia and abortions [36]. The time course of the antimicrobial effect of the $C_3(LA)_2$/$Lch_{AL1.1}$ (M80:20) was followed by a viable cell count. When *E. coli* O157:H7 cells were treated at the MIC concentration (6.25 µM), an effective reduction of viability (87.5%) was found after 30 minutes of treatment reaching a maximum (99.99%) after 120 min (Fig. 3, Table 4). When treated with each of the components of the binary system separately at the equivalent concentration, the geminal arginine surfactant $C_3(LA)_2$ (5 µM) produced a decrease of viability of 53.4% after 30 minutes of treatment. This effect was time dependent, increasing to 61.0% at 60 min (Table 3a) being 76.1% after 120 minutes. As expected, no antimicrobial effect was found for $Lch_{AL1.1}$ (1.5 µM). These results are consistent with the antimicrobial synergy (FIC =0.04) found between both compounds at the ratio M80:20 (Table 3). The binary system clearly produces a higher loss of viability in a shorter treatment time.

A different effect was observed in the case of *L. monocytogenes*, when the bacterial population was treated with the binary system at MIC concentration (6.25 µM). As expected, the $C_3(LA)_2$/$Lch_{AL1.1}$ (M80:20) exhibited higher antimicrobial activity than the individual components; a reduction of 44.1% viability was found after 30 min of treatment, which slowly increased to 99.8% after 120 min of contact (Table 3b, Table 4). When applied separately at the concentration of the mixture, the maximum effect of $C_3(LA)_2$ was 26.5% at 30 min of contact increasing to 59.0% after 60 minutes (Table b) reaching 84.8% reduction after 120 min of contact. No effect was observed with lychenysin. These results are accordance with the structural characteristics of the assayed

bacteria, the effects of the treatment being higher and faster in *E. coli* (Gram-negative) than *L. monocytogenes* (Gram-positive).

3.5. Flow cytometric (FC) analysis of the population of E. coli O157:H7 and L. monocytogenes after treatment with the $C_3(LA)_2$/$Lch_{AL1.1}$ (80:20) mixture.

The cell damage produced by the binary system M80:20 and the controls, $C_3(LA)_2$ and $Lch_{AL1.1}$, is presented in Table 4. When bacteria treated with any of the compounds assayed, the binary system or the individual components, three subpopulations of cells were observed: *i*) an unstained population, labelled in grey, corresponding to intact cells (D3); *ii*) a second subpopulation labelled in green (BOX-stained), corresponding to depolarized cells (D4); and *iii*) a third subpopulation of cells, labelled in red, which retained PI, indicating permeabilized cells, i.e. severely damaged cells (D1, D2).

E. coli O157:H7 cells were considerably disturbed, as M80:20 had a significant effect on membrane potential after 60 minutes of treatment at the MIC concentration (6.25 μM) compared with the negative control. 62.4 % of the population had the membrane depolarized (BOX-stained cells), which suggests a blockage in the respiratory chain as shown in Table 4. In contrast, exposure to pure $C_3(LA)_2$ (Fig. 4) or $Lch_{AL1.1}$ had no notable effect on membrane potential: the proportion of BOX-stained cells was 3.8 and 1.3 %, respectively. The most damaged cells, those with a permeabilized membrane (PI stained cells), reached 46.8 % after 60 min of contact (Table 4). Exposure to pure $C_3(LA)_2$ and $Lch_{AL1.1}$ had a negligible effect on membrane permeability, the proportion of PI-stained cells being only 1.1% (Figure 4) and 1.6 % (Table 4). The strongest effect on cell reduction viability (100%) was caused by the M20:80 mixture after 60 min of contact, whereas with $Lch_{AL1.1}$ only 1% loss of viability was observed (Table 4). However, divergences were seen with pure $C_3(LA)_2$: after 60 min of contact, the viability reduction was approximately 61 %, while only 4.9 % of affected cells were detected by FC (Table 4). This considerable disparity suggests that $C_3(LA)_2$ at an equivalent concentration to the mixture induced a loss in viability by a mechanism different to that evaluated by FC.

The response of the *L. monocytogenes* population to treatment with $C_3(LA)_2$, $Lch_{AL1.1}$ and M20:80 was also analysed (Table 4, Fig. 5). At the MIC (6.5 μM), M20:80 depolarized 38.4 % of cells. In contrast, the effect of $C_3(LA)_2$ and $Lch_{AL1.1}$ on the

membrane potential was low, being 8.8% and 4.3 % respectively. The maximum effect of M80:20 on membrane permeability was observed after 60 min of contact, when 64.4% of cells were BOX-stained and PI-stained. Exposure to $C_3(LA)_2$ and $Lch_{AL1.1}$ had little effect on membrane permeability; the proportion of PI-stained cells was 8.2% and 14.4 % (Table 4) respectively. It is noteworthy that although only 17% of cells were visibly affected by $C_3(LA)_2$, the reduction of viability was 60% (Table 4), suggesting an unspecific cell damaging effect associated with metabolic activity but not detected by FC. When compared with the results against *E. coli* O157:H7, the inhibiting effect of M80:20 was clearly lower against Gram-positive bacteria. The plate counts for both bacteria confirm that the antimicrobial-led alterations observed by FC, i.e., loss of membrane functionality and inhibition of respiratory activity, can result in cell death.

The proposed primary mode of antimicrobial action of lipopeptides is pore formation in membranes, leading to an imbalance of transmembrane ion flux and cell death [37, 38]. Recently, lichenysin interaction with a DPPC-model membrane was demonstrated, indicating that lichenysin penetrates inside the membrane [39]. Despite the low percentage of affected cells detected by bacterial count and by flow cytometry the present work assess the synergistic role of lichenysin, at low concentration, in the antimicrobial activity of the binary system with $C_3(LA)_2$.

3.6. Potassium ion leakage from E. coli O157:H7 and L. monocytogenes cultures

To determine changes in cell membrane permeability, K^+ leakage from *E. coli* O157:H7 and *L. monocytogenes* was examined during exposure to the M80:20, lichenysin and $C_3(LA)_2$. This approach is used to study antimicrobial effect on membrane integrity [2, 24, 40]. K^+ is the most abundant intracellular cation in all living organisms, including bacteria, and is essential for many cellular functions.

E. coli O157:H7 cells showed some leakage of intracellular K^+ in response to M80:20 and $C_3(LA)_2$ but no leakage was detected with lichenysin (Fig. 6a). The amount of extracellular K^+ after 15 min of contact was 0.26 and 0.34 ppm, respectively, which was lower than in the thermally treated population (0.81 ppm). In the case of *L. monocytogenes*, intracellular K^+ leakage after exposure to M80:20 and $C_3(LA)_2$ is shown in Figure 6b. Exposure to M80:20 after 15 min produced a K^+ concentration of 0.1 ppm

in the supernatant, whereas with $C_3(LA)_2$ it was 0.12 ppm, less than with the heat treatment (0.60 ppm). These results demonstrate that binary system induced leakage of intracellular K^+ from *E. coli* O157:H7 cells and to a lesser extent in *L. monocytogenes*. Dissipation of the K+ gradient across the cell membrane is a consequence of membrane damage and breakdown of the permeability barrier. K^+ leakage has been reported as higher in *Salmonella* Thiphymurium than in *S. aureus* treated with an arginine-derived surfactant [40]. Our results suggest that the biocide mechanism of action affects the cellular membrane with subsequent loss of intracellular K^+, although the binary system did not increase the K^+ leakage.

3.7. Transmission Electron Microscopy (TEM) of E. coli O157:H7 and L. monocytogenes

The effect on bacterial ultrastructure was assessed using TEM. Electron micrographs of *E. coli* O157:H7, used as a control, show a dense and compactly structured membrane. After exposure to 5 μM $C_3(LA)_2$, part of the *E. coli* O157:H7 population showed multiple alterations in the cytoplasm (Fig. 7a). Intracytoplasmic white regions and collapse of the cytoplasm were observed, although it should be stressed that membrane integrity was apparently maintained. The collapse of the cytoplasm could explain the reduction of viability without evidence of physical disintegration of the membrane (Table 4). In contrast, M80:20 caused major structural changes in *E. coli* O157:H7 cells (Fig. 7b). Due to the breakdown of the cytoplasmic membrane, leakage of the cytoplasm was observed outside the cells. The mixture caused a far greater effect than $C_3(LA)_2$ alone, not only in terms of changes in the cytoplasm, but in the degree of membrane damage.

Electron micrographs of *L. monocytogenes*, used as a control, depict a dense and compact membrane structure, as well as a thick peptidoglycan. The surfactant $C_3(LA)_2$ caused the formation of clearly visible mesosomes (Fig.8a), but the cell structure and form was not affected. Nevertheless, 69.3% reduction in viability was found (Table 4), suggesting that the changes produced in *L. monocytogenes* by M80:20 were critical. Figure 8b shows an alteration in cell morphology, possibly related to the loss of peptidoglycan rigidity, but only a low amount of cytoplasmic material was leaked. Thus, more cellular damage was caused by the $C_3(LA)_2/Lch_{AL1.1}$ (M80:20) than by $C_3(LA)_2$ alone in both strains; this observation is consistent with the results obtained by FC and

plate count. $Lch_{AL1.1}$ did not affect the integrity of the cell envelopes in *E. coli* O157:H7 and *L. monocytogenes* or the cell viability within the concentrations tested.

Similar results were found with the bis(Na-caproyl-L-arginine)-1,3-propanediamine dihydrochloride surfactant ($C_3(CA)_2$), which induces loss of membrane integrity in *E. coli* ATCC 10536, while in *S. aureus* ATCC 91444 lysosome formation and cytoplasm precipitation zones were observed [41] .Treatment with $C_3(LA)_2$ alone did not produce critical structural damage in the cell envelopes of *E. coli* O157:H7 in contrast with those reported with $C_6(LL)_2$ which produced breakage of the membrane leading to a massive lysis of the culture[19]. The ultrastructural changes observed in the case of *L. monocytogenes* were found also in *S. aureus* when treated with $C_6(LL)_2$ or other aminoacid-derived surfactants, changes in the morphology of the cells and mesosomes formations [19]

The trend for using compatible agents such as amino acid-derived surfactants in pharmaceutical or food industry formulations [42] may be reinforced by the use of co-surfactants to enhance antimicrobial properties. $Lch_{AL1.1}$ improved the antimicrobial activity of the gemini arginine surfactant $C_3(LA)_2$, mainly against Gram-negative bacteria. This suggests a potential application for this lipopeptide as a surfactant and antimicrobial ingredient in formulations. Indeed, the antimicrobial activity of essential oils is increased with emulsification mediated by rhamnolipids [43].

The results indicate that the binary system (M80:20) caused a loss of cell viability and disruption of the cell wall. The antimicrobial synergism between $C_3(LA)_2$ and $Lch_{AL1,}$ may be explained considering the strong interaction previously observed, where suggested a "pseudo-surfactant" formation. This "pseudo-surfactant" could produce a stronger hydrophobic interaction with lipid bilayer, besides the stronger electrostatic interaction, given by guanidine group, unique positively charged group, present in the mixture and acting as similar to cationic surfactant.

4. Acknowledgements

This work was financed by the Scientific and Technological Research Council, Spain, grants CTQ2014-59632-R, CTQ2013-41514-P and MAT2012-38047-CO2-02 and by the

IV Pla de Recerca de Catalunya (Generalitat de Catalunya), grant 2014SGR-534. We thank Ecuador's Government for a SENESCYT-ESPOL grant.

5. References

[1] D.H. Sasseville, Dermatol. Ther, 17 (2004) 251-263.

[2] D.S. Orlov, T. Nguyen, R.I. Lehrer, J. Microbiol. Methods 49 (2002) 325-328.

[3]. F. Rivardo, H. Ceri, Int. J. Antimcrob Agents, 37 (2011) 324-331.

[4] I. Galani, K. Orlandou, H. Moraitou, G. Petrikkos and M. Souli, Int. J. Antimicrob. Agents, 43 (2014) 370-374.

[5] L. Saiman, Paediatr. Respir. Rev, 8 (2007) 249-255.

[6] A.M Carmona-Ribeiro, L. Días de Melo Carrasco, Int. J. Mol Sci 15 (2014) 180040-1883.

[7] C. Chaouat, Ch. Roques S. Franceschi-Messant, E. Perez, I. Rico-Lattes, J.Surfact. Deterg, 16 (2013) 717-722.

[8] N. Lozano, R. Pons, A. Pinazo, Diacyl glycerol arginine-based surfactants: biological and physicochemical properties of catanionic formulations, Amino Acids Amino Acids 40 (2011) 721-729.

[9] I.M. Banat, I. Gandolfi, G. Bestetti, M.G. Martinotti, L. Fracchia, T.J. Smyth, R. Marchant, Appl. Microbiol. Biotechnol., 87 (2010) 427-444.

[10]. L. Rodrigues, J. Texeira, R. Oliveira, , J. Antmicrob. Chemother, 57 (2006) 609-618.

[11] M.M. Yakimov, K.N. Timmis, V. Wray, H.L. Fredrikson, Appl Environ Microbiol, 61 (1995) 1706-1713.

[12] E.J. Gudiña, R. Sen, L.R. Rodrigues, Trends Pharmacol, 34 (2013) 667-675.

[13] L.R. Rodrigues, Adv. Exp. Med. Biol, 715 (2011) 351-367.

[14] R. Marchant, Trends Biotechnol 30 (2012) 558-565.

[15] A. Colomer, M.A. Manresa, M.P. Vinardell, M. Mitjans, M.R. Infante, L. Pérez, J. Med. Chem, 54 (2011) 989-1002.

[16] A. Pinazo, L. Pérez, M.R. Infante, Ind. Eng. Chem. Res, 50 (2011) 4805-4817.

[17] L. Perez, A. Manresa, C. Solans, M.R. Infante, Langmuir, 12 (1996) 5296-5301.

[18] J. Coronel-León, A. Grau-Campistany, M. Farfan, F. Rabanal, A. Manresa, A.M. Marqués, Ann. Microbiol, 65 (2015) 2065-2078.

[19] A. Colomer, L. Pérez, R. Pons, M.R. Infante, D. Perez-Clos, A. Manresa, M.J.Espuny and A. Pinazo, Langmuir, 29 (2013) 7912-7921.

[20]. E. Haba, R. Pons, L. Pérez, A. Manresa, , Biochim. Biophys. Acta, 1838 (2014) 776-783.

[21] J.H. Jorgensen, Susceptibility test methods: dilution and disk diffusion methods in: J.J. Murray PR Baron EJ, Landry HL, Pfaller MA, (Ed.) Manual of Clinical Microbiology, 9th ed, ASM Press, Washington, DC., 2007, pp. 1152-1172.

[22] C. Stefaniu, H. Möhwald, , Adv. Colloid Interface Sci, 208 (2014) 197-213.

[23] D. Schwartz, Méthodes statistiques à l'usage des medicins et des biologists, Flamarion Medecine Sciences. Paris., 1963.

[24] S. Bouhdid, M. Amensour, A. Zhiri, M.J. Espuny, A. Manresa,, J. Appl. Microbiol, 109 (2010) 1139-1149.

[25] A. Pinazo, L. Pérez, M.R. Infante, E.I. Franses,, Langmuir, 15 (1999) 3134-3142.

[26] D. Weihs, A. Pinazo-Gassol, L. Pérez, E.I. Franses, Y. Talmon., Colloids Surfaces A Physicochem. Eng. Aspects, 255 (2005) 73-78.

[27]. P. Jauregi, L. Catiau, D. Lecouturier, P. Jacques, , Sep. Purif. Technol., 104 (2013) 175-182.

[28] J. Arutchelvi, Philip, M. Doble, Colloids Surf. B. Biointerfaces, 116 (2014) 396-402.

[29] P. Das, R. Sen, J. Appl. Microbiol., 104 (2008) 1675-1684.

[30] A. Carmona-Ribeiro and L. Dias de Melo Carrasco, Int. J. Mol. Sci, 15 (2014) 18040-11883.

[31] D. Song, S. Liang, J. Wang, Colloids Surfaces A Physicochem. Eng. Aspects, 436 (2013) 201-206.

[32] T. Imura, T. Taira, T. Morita, T. Fukuoka, K. Aburai, H. Sakai, M. Abe, D. Kitamoto, J. Oleo Sci, 73 (2013) 67-73.

[33] L. Magalhães, Food Control, 29 (2013) 138-142.

[34] K. Joshi-Navare, A. Prabhune, Biomed Res. In, (2013) 1-8.

[35] F. Fathi, N. Wang, C. Xiang, R. Love, Z. She, H.B. Kraatz, Biosens. Bioelectron, 58 (2014) 193-199.

[36]L.V. de Araujo, U. Lins, L.M.M.Santa-Anna M. Nitschke, D.G.M. Freire, Food Res. Int., 44 (2011) 481-488.

[37] C.L. Bender, F. Alarcón-Chaidez and D.C. Gross, Microbiol. Mol. Biol. Rev, 63 (1999) 266-292.

[38] R.H. Baltz, Curr. Opin. Chem. Biol., 13 (2009).

[39] J. Coronel, J.A. Teruel, A.M. Marqués, A. Manresa, A. Ortiz, Langmuir 32 (2016) 78-87.

[40] E. Rodriguez, X. Rocabayera, A. Manresa, J. Appl Microbiol, 96 (2004) 903-912.

[41] J.A. Castillo, M. R. Infante, J. Comas , A. Manresa,, J. Antimicrob. Chemother, 57 (2006) 691-698.

[42] A. Pinazo, A.M. Marqués, M. Bustelo, M.J. Espuny, L. Pérez, Adv. Colloid Interface Sci., 229 (2015) 17-39.

[43] E. Haba, N. Torrego-Solana, A.M. Marqués, M.J. Espuny, M.J. García-Celma, A. Manresa, Int. J. Pharm, 476 (2014) 134-141.

Figure 1. Structures (A) $Lch_{AL1.1}$ and (B) $C_3(LA)_2$, $C_6(LL)_2$ compounds.

Figure 2. π-A Compression isotherms. a) pure $C_3(LA)_2$ surfactants, $Lch_{AL1.1}$ and binary mixtures (M 80:20 and M 50/50) of $C_3(LA)_2/Lch_{AL1.1}$. b) pure $C_6(LL)_2$ surfactants, $Lch_{AL1.1}$ and binary mixtures (M 80:20 and M 50/50) of $C_6(LL)_2/Lch_{AL1.1}$. The subphase was Tris (pH = 7.4).

Figure 3. Reduction of cell viability (cfu/ml) versus time: (a) *E. coli* O157:H7 (B) *L. monocytogenes*. $C_3(LA)_2$ (5 μM) (□); $C_3(LA)_2$/ $Lch_{AL1.1}$ (80:20) MIC (Δ) and $Lch_{AL1.1}$ (1.25 μM) (◊). The data correspond to the average of three independent experiments ± SE (error bars).

Figure 4. Dual parameter of *E. coli* O157:H7 stained cells (BOX and PI) caused by exposure to $C_3(LA)_2$ /$Lch_{AL1.1}$ (80:20) and $C_3(LA)_2$ (a) cells treated with $C_3(LA)_2$ at the concentration in the mixture (5 μM) (b) cells treated with $C_3(LA)_2$ /$Lch_{AL1.1}$ (M80:20) at MIC concentration (6.25μM). In all cases, time of contact was 1 h.

Figure 5. Dual parameter of *L. monocytogenes* stained cells (BOX and PI) caused by exposure to $C_3(LA)_2$ /$Lch_{AL1.1}$ (80:20), $C_3(LA)_2$ and $Lch_{AL1.1}$. (a) cells treated with $C_3(LA)_2$ at the concentration in the mixture (5 μM), (b) cells treated with $C_3(LA)_2$ /$Lch_{AL1.1}$ (80:20) at MIC concentration (6.25 μM). In all cases, time of contact was 1 h

Figura 6. Potassium leakage of the cell suspension of (a) *E. coli* O157:H7 and (b) *L. monocytogenes* exposed to $C_3(LA)_2$ 5 µM (●);$C_3(LA)_2/Lch_{AL1.1}$ (80:20) MIC(■); exposure to 70ºC (▲) acted as positive control. $Lch_{AL1.1}$ doesn´t cause potassium leakage.

Figure 7. Effect on membrane ultrastructure of *E. coli* O157:H7 caused by exposure to $C_3(LA)_2$/ $Lch_{AL1.1}$ (M80:20) at CMI concentration (6.5 µM) and $C_3(LA)$ at the proportion in the mixture (5 µM), shown by transmission electron microscopy. a) $C_3(LA)_2$ 5 µM, (50X) and b) $C_3(LA)_2/Lch_{AL1.1}$ (M80:20) (50X). In all cases, time of contact was 120 min.

Figure 8. Effect on membrane ultrastructure of *L. monocytogenes* caused by exposure to $C_3(LA)_2$/ $Lch_{AL1.1}$ (M80:20) and $C_3(LA)_2$ at the corresponding MIC concentration, shown by transmission electron microscopy. a) $C_3(LA)_2$ 5 µM, (50X) and b) $C_3(LA)_2/Lch_{AL1.1}$ (M80:20) (50X). In all cases, time of contact was 120 min.

Figure 1

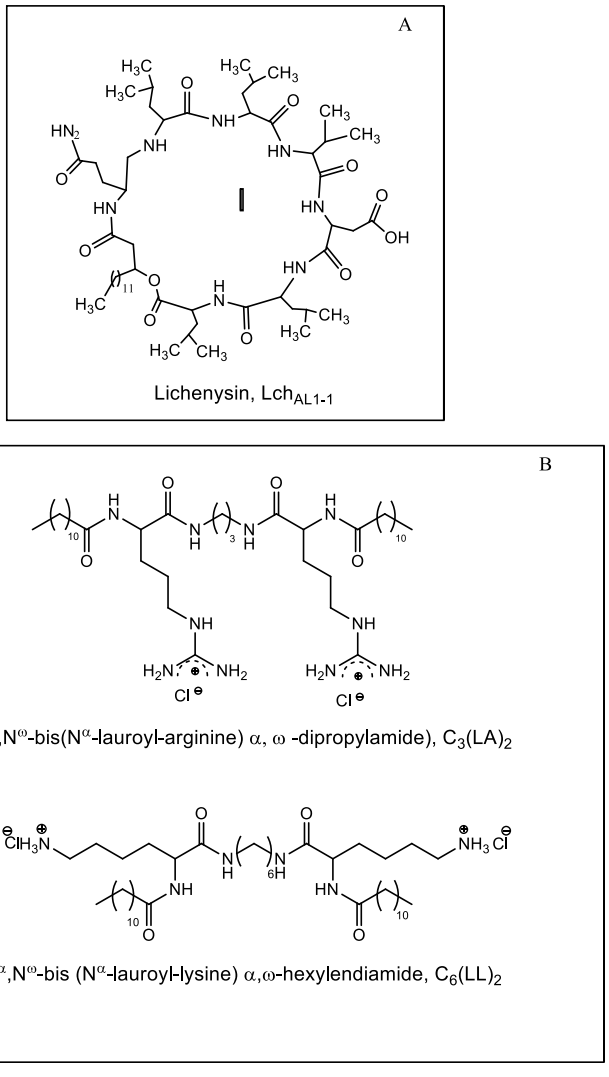

Figure 2.

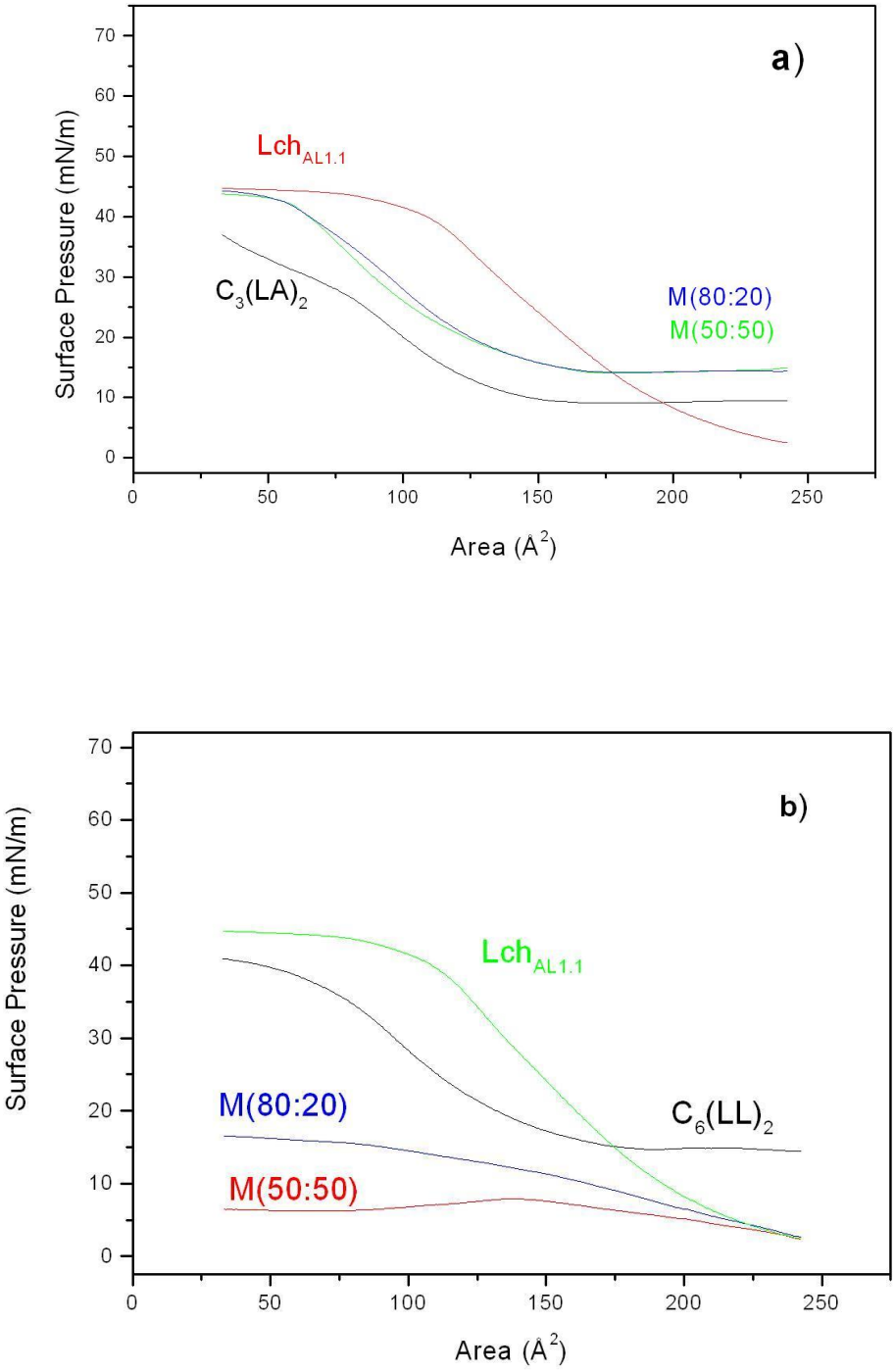
a)
Lch$_{AL1.1}$
C$_3$(LA)$_2$
M(80:20)
M(50:50)
Surface Pressure (mN/m)
Area (Å^2)
0
10
20
30
40
50
60
70
0
50
100
150
200
250
b)
Lch$_{AL1.1}$
M(80:20)
M(50:50)
C$_6$(LL)$_2$
Surface Pressure (mN/m)
Area (Å^2)

Figure 3

a) ***E. coli***

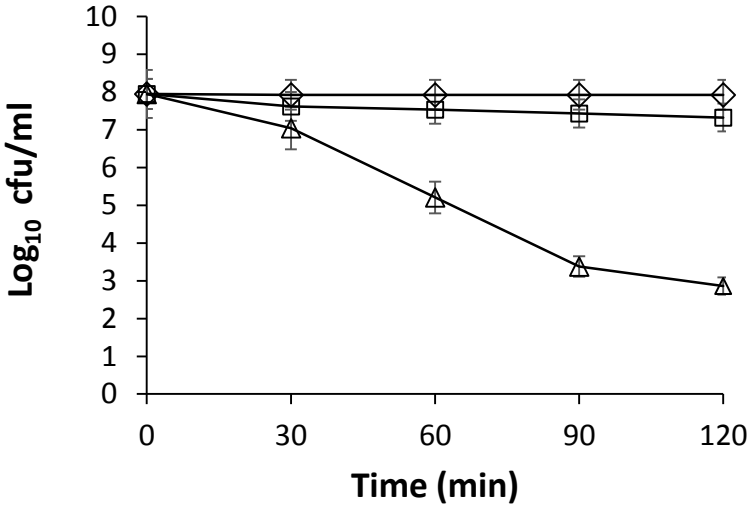

L. monocytogenes

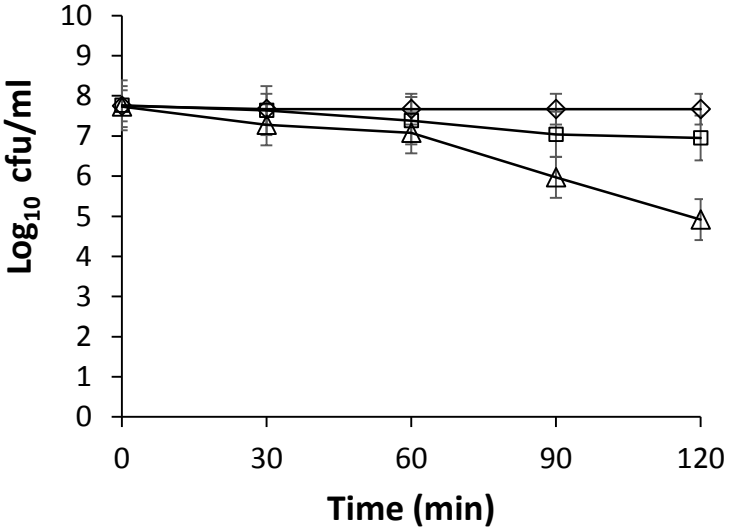

Figure 4.

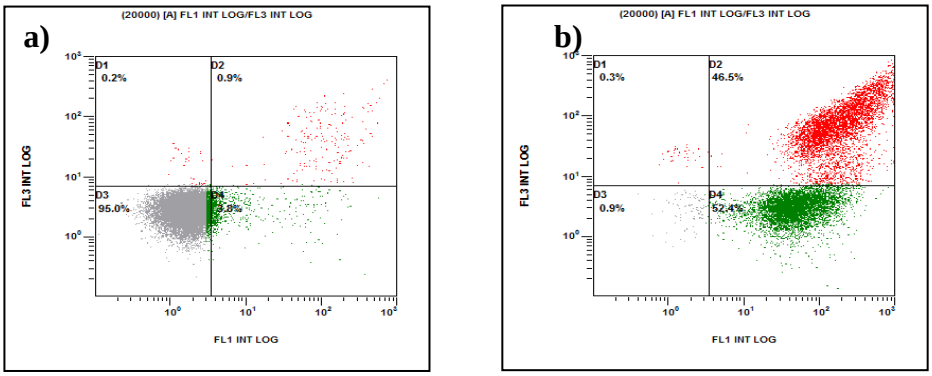

Figura 5.

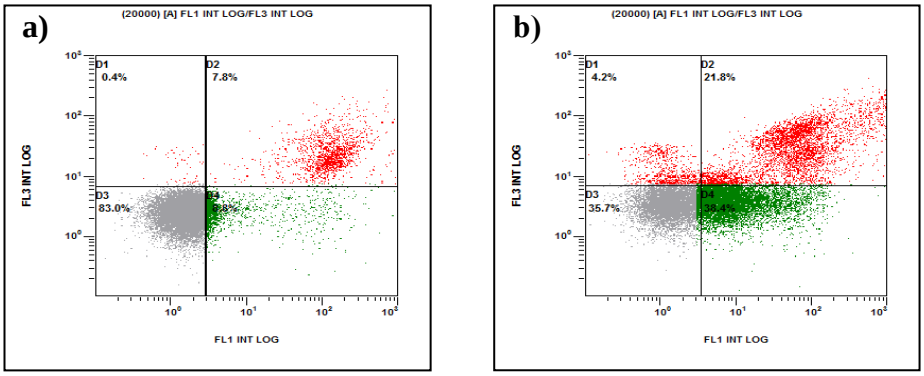

Figure 6.

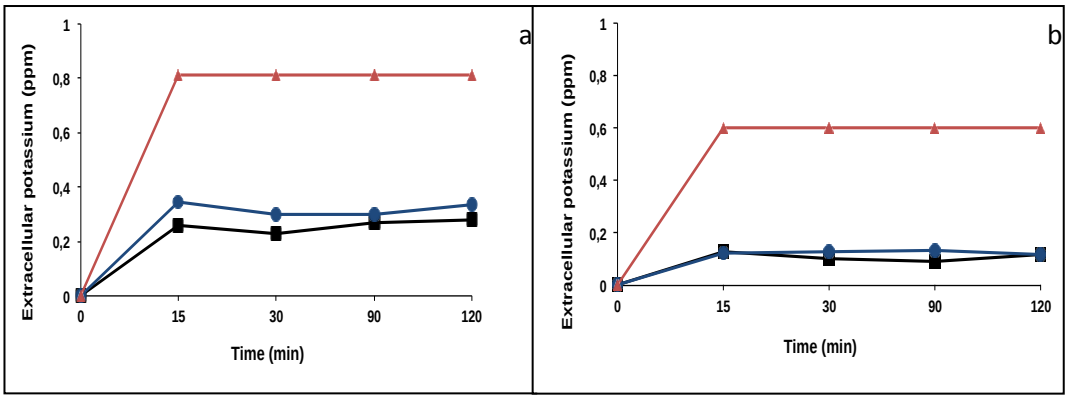

Figure 7.

a)

b)

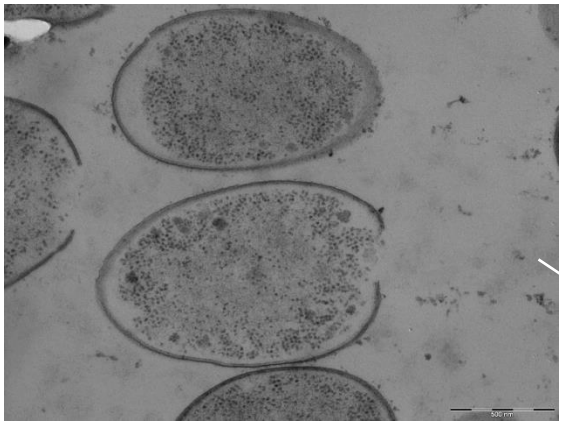

Figure 8.

a)

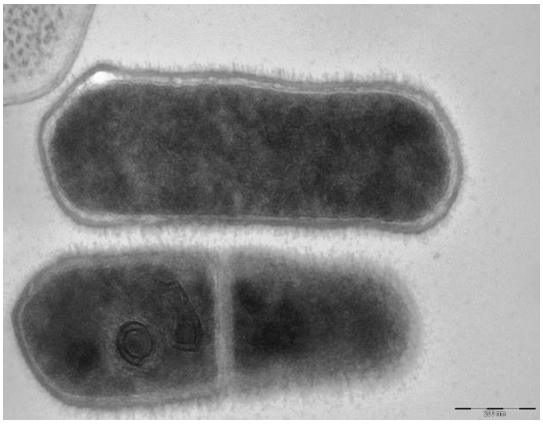

b)